MNRAS **000**, 000–000 (0000) Preprint 14 February 2018 Compiled using MNRAS LATEX style file v3.0

Lyman-alpha spectra from rotating outflows

Maria Camila Remolina-Gutiérrez[1] ⋆ & Jaime E. Forero-Romero [1] †
[1] *Departamento de Física, Universidad de los Andes, Cra. 1 No. 18A-10 Edificio Ip, CP 111711, Bogotá, Colombia*

14 February 2018

ABSTRACT
Outflows and rotation are two ubiquitous kinematic features in the gas distributions of galaxies. We perform Monte Carlo radiative transfer simulations of outflowing gas with additional solid body rotation to understand how these two features impact the morphology of the Lyman-α emission line. One of the most notorious results is that rotation increases the detected flux at the line's center in comparison with the non-rotational case. Rotation also induces a line broadening and a dependency with the viewing angle. We present a semi-analytic model that modifies the spectra of non-rotational that manages to reproduce the main features of these Monte Carlo simulations.

Key words: galaxies: dwarf — radiative transfer — Methods: numerical

1 INTRODUCTION

The interpretation of the Lyman-α emission in galaxies is key to understand their evolutionary processes (Partridge & Peebles 1967). Recent improvements in instrumentation have revolutionized the kind of studies that can be performed on Lyman-α emitting galaxies (LAEs.) For instance, it is now possible to infer detailed kinematic maps for nearby galaxies. The study of these maps would allow us to build data-driven models to interpret the Lyα spectra of unresolved galaxies, helping us to constrain the physical conditions of the interstellar medium (ISM) processing the Lyα radiation.

These kinematic maps show that lyman alpha emitting galaxies have two overimposed velocity patterns: coherent rotation plus and a random motions around the mean value provided by rotation. Depending on the system under study, one of the two features can be more important, or they can be found in equal measure. These kinematic features play an important role in shaping the Lyα .

Models of the Lyα have also shown that there is clear signal for outflowing gas most probably produced by star formation activity. The characteristic signal for these outflows is the asymmetrical Lyα linea with a more pronounced read peak.

The effects of either outflows or rotation on the Lyα line have been already explored. Here e present for the first time a study of the joint effects of galaxy outflows and rotation, two of the three major kinematic components expected in LAEs.

⋆ mc.remolina197@uniandes.edu.co
† je.forero@uniandes.edu.co

We study a simplified geometrical configuration corresponding to a spherical gas cloud with symmetrical radial outflows and a rotation profile corresponding to a solid body. We base our modeling on a Monte-Carlo radiative transfer code called CLARA (Code for Lyman Alpha Radiation Analysis) presented for the first time by Forero-Romero et al. (2011).

Besides modeling the impact of joint rotation and outflows, we also check to what extent the analytical model presented by Garavito-Camargo et al. (2014) to explain the effects of rotation can also be applied in our case. We show that solid body rotation effects can be included in the results of other radiative transfer model in the case of large optical depths. In this case it is a good approximation to Doppler boost the results of the model without rotation.

The structure of the paper is the following. We introduce first our theoretical tools and assumptions in Section 2. We continue in Section 3 with the results from the Monte-Carlo simulation, the comparison against the semi-analytical approximation which we use to make a thorough exploration of the effect of rotation. In Section 4 we discuss our results and their possible implications for observational analysis to finally present our conclusions in Section 5.

2 THEORETICAL MODELS

2.1 Monte-Carlo Radiative Transfer Model

CLARA follows the propagation of individual photons through a neutral Hydrogen medium characterized by its temperature, velocity field and global optical depth. The code assumes an homogeneous density throughout the simulated volume. In the current implementation we neglect

$\tau_{\rm H}$	$v_{\rm rot}$ (km s^{-1})	$v_{\rm out}$ (km s^{-1})
10^5	{0}	{5, 25, 50}
10^6	{0}	{5, 25, 50}
10^7	{0}	{5, 25, 50}
10^5	{50, 100}	{25, 50, 75}
10^6	{50, 100}	{25, 50, 75}
10^7	{50, 100}	{25, 50, 75}

Table 1. Parameters' Values. List of values that were used to construct the radiative transfer models. Values in braces for a row indicate that all possible combinations in of $\tau_{\rm H}$, $v_{\rm rot}$ and $v_{\rm out}$ are used.

the influence of dust. Our basic models is an spherical distribution of neutral hydrogen, an approximation commonly used in the literature, as it explains a wide variety of observational features (Ahn et al. 2003; Verhamme et al. 2006; Dijkstra et al. 2006).

The central element in this paper is the velocity field that captures outflows and rotation. Outflows are captured by a Hubble-like radial velocity profile with the velocity magnitude increasing linearly with the radial coordinate; the outflow model is fully characterized by $V_{\rm out}$, the velocity at the sphere's surface. Rotation follows a solid body rotation profile, which is fully characterized by $V_{\rm rot}$, the linear velocity at the sphere's surface.

The total velocity field corresponds to the superposition of rotation and outflows. The cartesian components take the following form:

$$v_x = \frac{x}{R}V_{\rm out} - \frac{y}{R}V_{\rm rot}, \quad (1)$$

$$v_y = \frac{y}{R}V_{\rm out} + \frac{x}{R}V_{\rm rot}, \quad (2)$$

$$v_z = \frac{z}{R}V_{\rm out}, \quad (3)$$

where x, y and z are the cartesian position coordinates with the origin at the sphere's center, R is the radius of the sphere and the direction of the angular velocity vector corresponds to the $\hat{k}$ unit vector.

For each model setup we follow 10^5 individual photons generated at the center of the sphere at the Lyα line's center as they propagate through the volume and finally scape. We store the final frequency and propagation direction for each photon at its last scattering.

In Table 1 we list the combination of $\tau_{\rm H}$, $v_{\rm rot}$ and $v_{\rm rot}$ values used in this paper. The range of values have some overlap with the expectations from a dwarf galaxy with a total neutral hydrogen mass of 10^8-10^9 $M_\odot$. We run a total of 24 different models.

2.2 Analytical Model for Bulk Rotation

Rotation induces two main effects on the Lyα line morphology. First. Break of spherical symmetry due to the preferential direction introduced by the rotation axis. This symmetry break is reflected in the observed spectra as a dependency on the viewing angle, θ, between the line of sight of a distant observer and the rotational velocity. Second. Line blurring as the rotational velocity increases. At a fixed viewing angle, faster rotation induces makes the observed line wider and increases the flux around the line's center.

Garavito-Camargo et al. (2014) presented in the Appendix an analytical model that accounts for these two features. The basic assumption of the analytical model is that each differential surface element on the sphere Doppler shifts the photons that it emits In this paper we introduce this ansatz by post-processing the results of the outflow simulations without rotation. This allows us to produce new Lyα spectra and compare them with the full radiative transfer solution including both outflows and rotation.

3 RESULTS

3.1 Monte-Carlo Radiative Transfer Model

We evaluate first the effects of increasing rotational velocity at fixed values of the optical depth and outflow velocity. Figure 1 summarizes the information. All plots correspond to the same outflow velocity of $\rm v_{out} = 50 km\ s^{-1}$, rows have constant optical depth and columns have constant rotational velocity. Each panel shows different morphologies corresponding to varying line-of-sight viewing angle.

We now evaluate the effects of increasing outflow velocity at fixed values for the optical depth and rotational velocity. Figure A2 summarizes the information following the same patters as Figure A1, only that this time all plots correspond to the same rotation velocity of $\rm v_{rot} = 50 km\ s^{-1}$.

3.2 Doppler Shifts to Include Rotational Effects

We know that rotation alone does have an impact on the Lyα line morphology and we get the same influence in it that previous works. Together with the outflows, we found that the resulting spectra is equivalent to a non-rotating galaxy with outflows that undergoes a Doppler Shift in velocity, weighted by amount of photons that if rotating would project their escape in $\hat{k}$'s direction. The formulas to calculate this shift are:

$$V' = V + \vec{v}_{\rm rot} \cdot \hat{k} = V + V_{\rm rot}(xk_x - yk_y) \quad (4)$$

where V' is the new Doppler shifted velocity, V is the velocity caused by outflows and $\vec{v}_{\rm rot} = V_{\rm rot}(x\hat{i} - y\hat{j})$.

Figure 3 displays this Doppler shift for four different configurations with a fixed optical depth $\tau_{\rm H}$. In each cell of the grid there is a Lyα spectrum for a galaxy with only outflows and two Lyα spectra for the galaxy with outflows and rotation, one obtained from the radiative transfer and the other by the Doppler shifting of the non-rotating galaxy.

In order to compare the line created with the radiative transfer process that involves the rotation (RT) and the line with only outflows that is Doppler shifted (DS), we calculate three main characteristics for each spectrum. We measure the line's mean velocity, standard deviation and skewness for both RT's and DS's approaches. We plot the results for each value in Figures 4, 5 and 6, respectively for $\tau_{\rm H} = 10^7$. We highlight that these 3 plots increase their fit tendency with

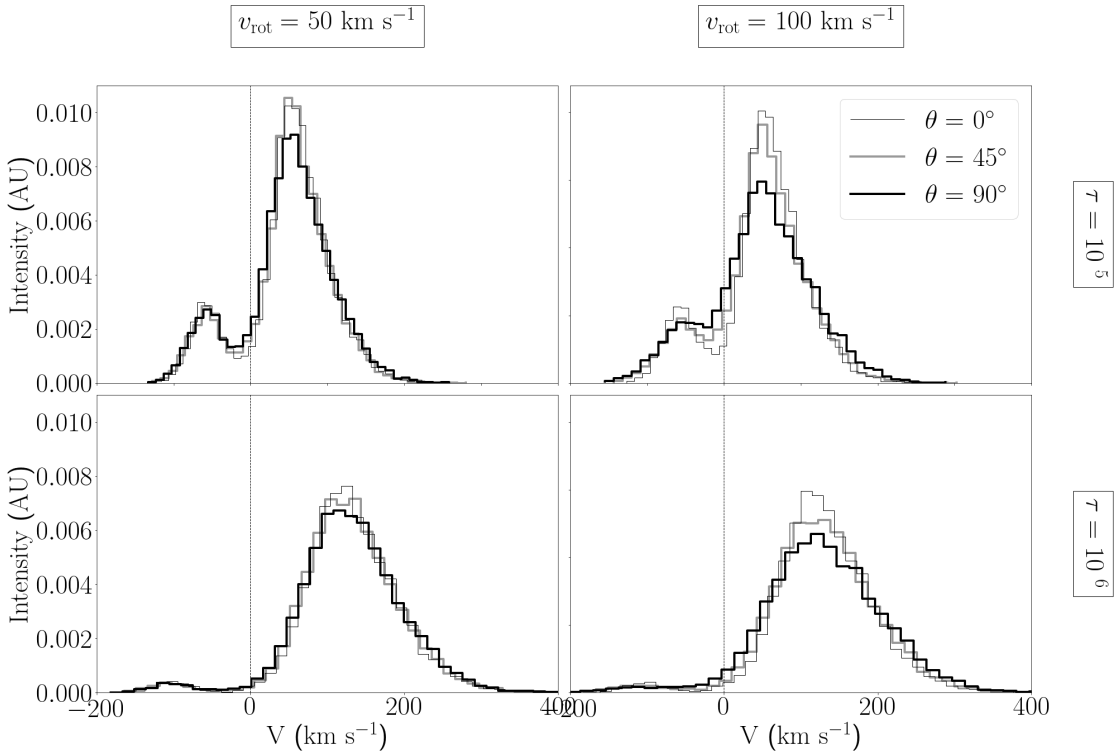

Figure 1. Spectra for fixed outflow velocity: We fixed $v_{\rm out}$ = 50km s^{-1}. We vary $v_{\rm rot}$ increasing from left to right, $\tau_{\rm H}$ increasing from top to bottom, and θ according to the legend.

a higher optical depth. The reasons why will be discussed in section 4.

This shows that the DS model can reproduce the main characteristics of the RT one. Because of this, we can introduce rotation effects in any spectra without running the radiative transfer simulations, that usually take a significant amount of time and computational resources.

In addition to this, we also evaluate the effects of the viewing angle for fixed rotational and outflows velocity. We measure the intensity of the valley between peaks, for each θ and $\tau_{\rm H}$. Figure 7 summarizes the information with all plots corresponding to the same outflow velocity of $v_{\rm out}$ = 75km s^{-1}and rotation velocity of $v_{\rm rot}$ = 50km s^{-1}.

4 DISCUSSION

4.1 Theoretical Insights

Why Doppler Shift works. Talk about radiative transfer... In Fig. 8 we present the spectrum pf a LAE taken from to different sides of the galaxy. As the LAE is rotating, one side is being redshifted while the other is blueshifted. We see that the combined spectrum is a weighted line, in black, that combines these past two. This shows that there is in effect a Doppler Shift and justifies our choice to apply it after the outflows spectrum is obtained.

A first approach to an analytical expression that returns the Lyα spectrum from a rotating galaxy is presented by Garavito-Camargo et al. (2014). This derivation is based on the assumption that the distribution of photons' propagation directions at the edge of the galaxy is anisotropic and depends of $\tau_{\rm H}$ only. So this approximation becomes more accurate with higher optical depth and it is also the reason why the Doppler Shift technique to induce rotational effects to an outflow Lyα spectrum works.

On the other hand, regarding the parameters $v_{\rm rot}$, $v_{\rm out}$, and θ for which this model would work, we have the following. The effect of the outflows velocity is much more sensitive on the spectrum than the rotational one; meaning that for a high $v_{\rm out}$, the $v_{\rm rot}$ value would have to be equal or greater in order to be able to glimpse the shift in frequency that rotation induces. Regarding θ, the introduction of rotation in the model implies that it will only affect galaxies with its viewing angle $\theta \neq 90°$. This can be observed in the cartesian components of the velocity of the atoms (Eq. 1, 2, 3) where the only velocity factor affecting v_z is the outflows one.

4.2 Application to observational data

We find three different approaches how this model can have observational implications. Firstly, as the resolution of astronomical instruments is increasing, new images from LAEs can be spatially resolved in a way that rotation velocities of the galaxy can be determined. New spectrographs like MUSE should help obtain kinematic information from LAEs by using our model. As for now, previous works in the literatures have already found useful data to support this idea. Fig 7 of Prescott et al. Prescott et al. (2015) shows the pres-

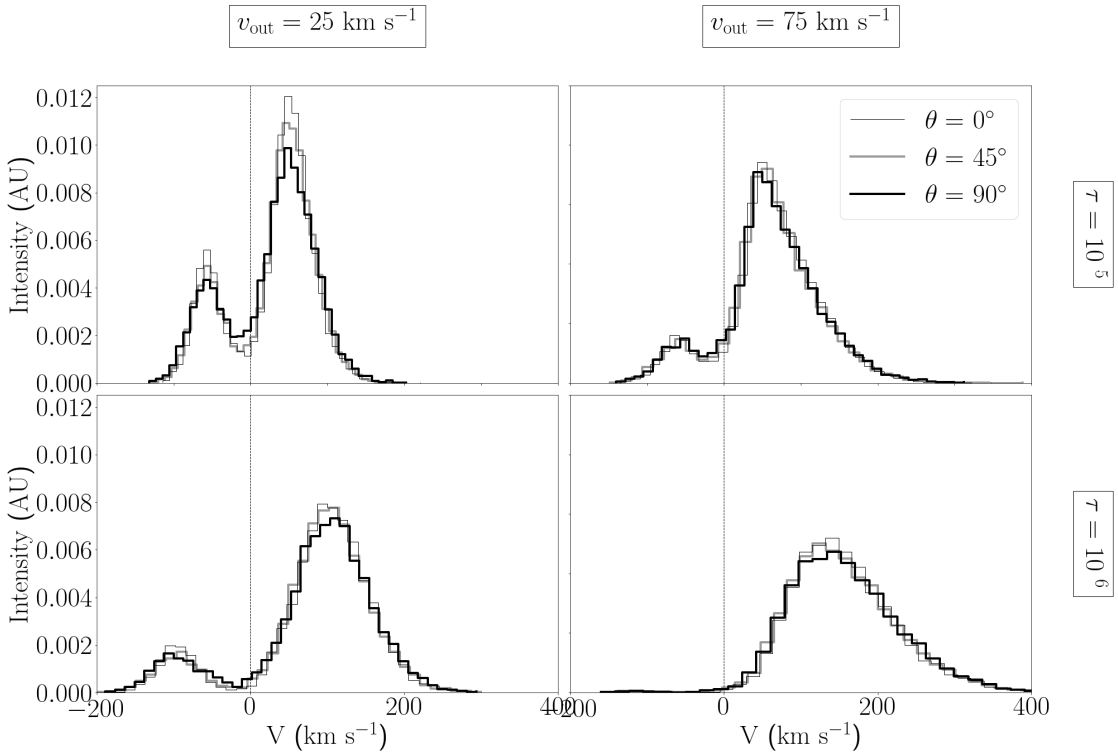

Figure 2. Spectra for fixed rotational velocity: We fixed v_{rot} = 50km s^{-1}. We vary v_{out} increasing from left to right, τ_H increasing from top to bottom, and θ according to the legend.

ence of Doppler shift and Herenz et al. (2016) creates 2D line of sight velocity maps of several LARS (Lyman Alpha Reference Sample) galaxies.

Another application of this new model to the current interpretation of Lyα spectra, is that the central ($V = 0$) emission of the spectra seen in the Lyα line, is a consequence of the viewing angle of the galaxy and can be controlled by it. Several authors have suggested that this central emission is caused by radiation that escapes the galaxy without scattering. So we present an alternative that solves this issue. In addition, the effect of outflows velocities v_{rot} in current models can modify the asymmetry of peaks present in the Lyα line. However the intensity of the valley and the width of the line were not easily reproduced. In this work we provide a tool to provide these effects with values of v_{out} and v_{rot} that do not exceed the typical LAEs' numbers found in the literature.

Kulas... Finally, we present a reconstruction of a selected Lyα spectrum presented by Kulas et al. (2012) and reproduced with the permission of the author. We create a fit of the Lyα line and predict its kinematic properties.

5 CONCLUSIONS

In this paper we create, for the first time, a computational model for LAEs that emulate the kinematic effects of galaxy rotation and outflows in the Lyα spectral line.

Our main conclusions are:

- The effect of rotation v_{rot} in a LAE spectrum is to broaden the Lyα line.
- The effect of outflows v_{out} in a LAE spectrum is to increase the peak asymmetry of the Lyα line.
- The effect of optical depth τ_H in a LAE spectrum is to induces a redshift around the zero velocity in the Lyα line.
- Rotation induces a dependency in viewing angle on the Lyα line. The closer the observer is to the equator of the galaxy, the higher is the central valley of the frequency distribution.
- Rotations induces a Doppler Shift in frequency of the only-outflow spectrum of the LAE.
- The final spectra obtained are roughly consistent with LAEs observations.

REFERENCES

Ahn S.-H., Lee H.-W., Lee H. M., 2003, MNRAS, 340, 863
Dijkstra M., Haiman Z., Spaans M., 2006, ApJ, 649, 14
Forero-Romero J. E., Yepes G., Gottlöber S., Knollmann S. R., Cuesta A. J., Prada F., 2011, MNRAS, 415, 3666
Garavito-Camargo J. N., Forero-Romero J. E., Dijkstra M., 2014, ApJ, 795, 120
Herenz E. C., et al., 2016, A&A, 587, A78
Kulas K. R., Shapley A. E., Kollmeier J. A., Zheng Z., Steidel C. C., Hainline K. N., 2012, ApJ, 745, 33
Partridge R. B., Peebles P. J. E., 1967, ApJ, 147, 868
Prescott M. K. M., Martin C. L., Dey A., 2015, ApJ, 799, 62
Verhamme A., Schaerer D., Maselli A., 2006, A&A, 460, 397

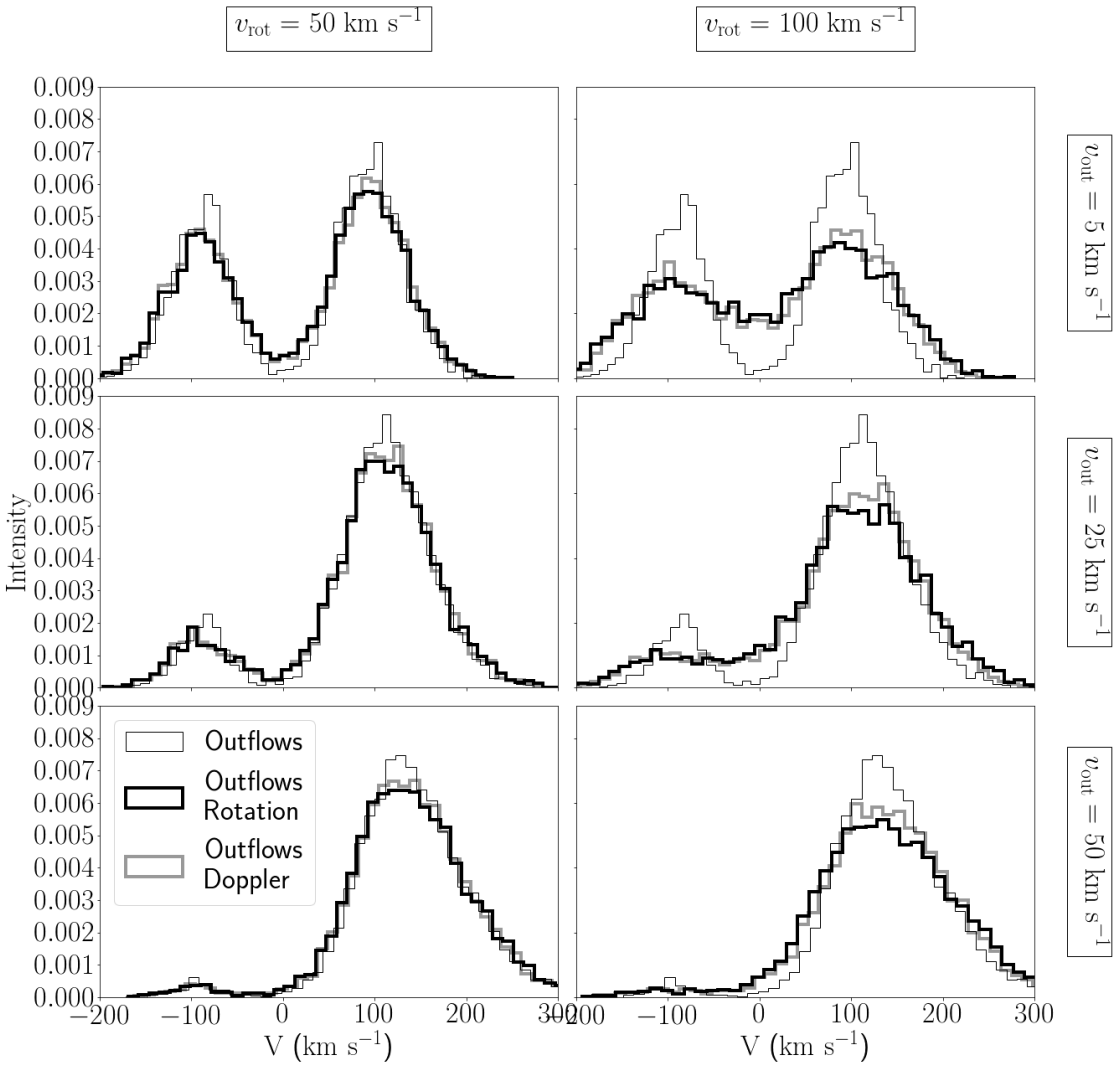

Figure 3. Doppler shift effect: We fixed $\tau_{\rm H} = 10^6$ and θ =?. We vary $v_{\rm rot}$ increasing from left to right and $v_{\rm out}$ increasing from top to bottom. The legend represents the Lyα line obtained if there is no rotation (in thin line), if there is a radiative transfer of rotation and outflows (thick and clear line), and if there is a radiative transfer of only outflows, but also a Doppler shift from the rotational velocity (thick and dark line).

APPENDIX A: ADDITIONAL FIGURES

In this appendix we show more Lyα spectra in the Figures A1 and A2 with more combinations of $v_{\rm rot}$ and $v_{\rm out}$.

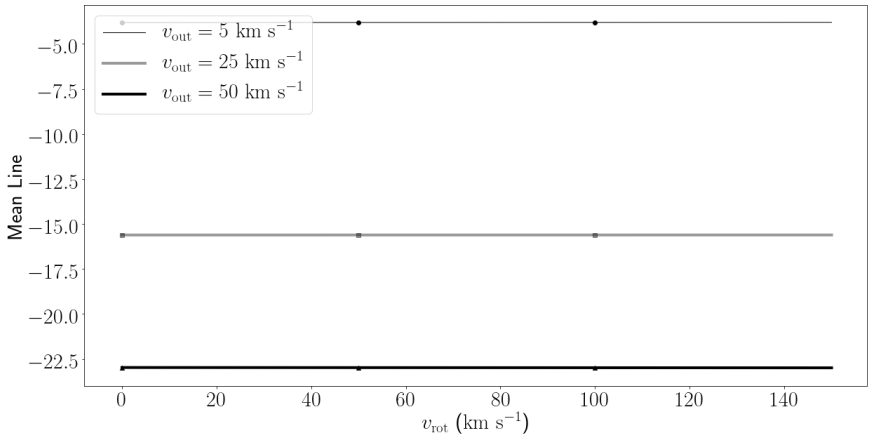

Figure 4. Mean line for RT and DS: The dots represent the Radiative Transfer and the lines represent the Doppler Shift. We fixed $\tau_{\rm H} = 10^7$.

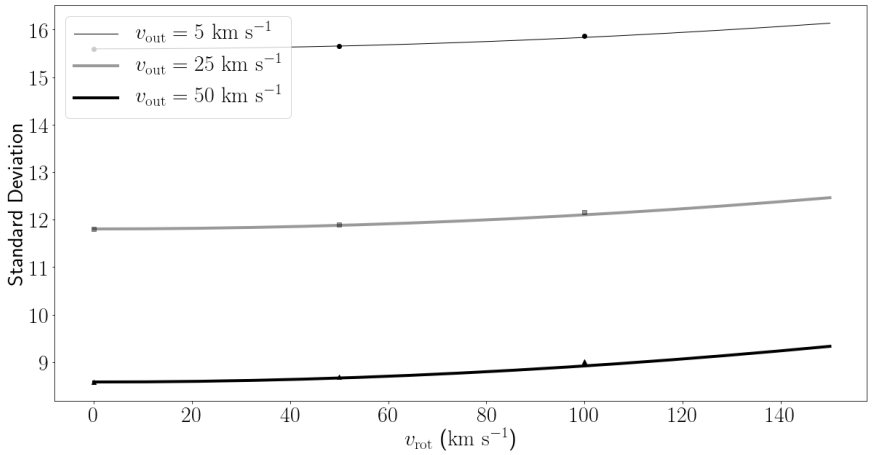

Figure 5. Standard Deviation for RT and DS: The dots represent the Radiative Transfer and the lines represent the Doppler Shift. We fixed $\tau_{\rm H} = 10^7$.

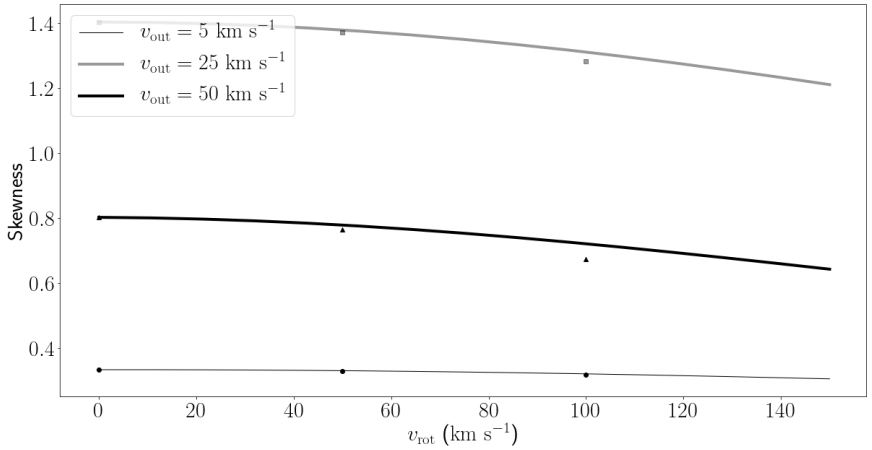

Figure 6. Skewness for RT and DS: The dots represent the Radiative Transfer and the lines represent the Doppler Shift. We fixed $\tau_{\rm H} = 10^7$.

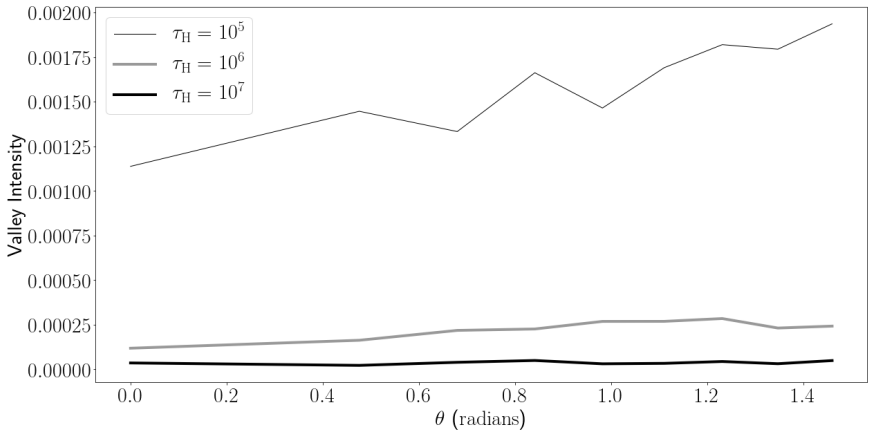

Figure 7. Caption: We fixed $v_{out} = 75$km s^{-1}and $v_{rot} = 50$km s^{-1}.

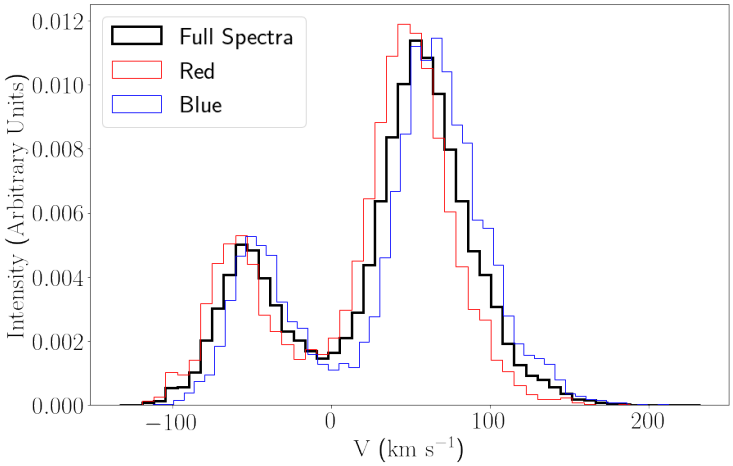

Figure 8. Caption: $v_{out} = 25$km s^{-1}, $v_{rot} = 100$km s^{-1}, $\tau_H = 10^5$.

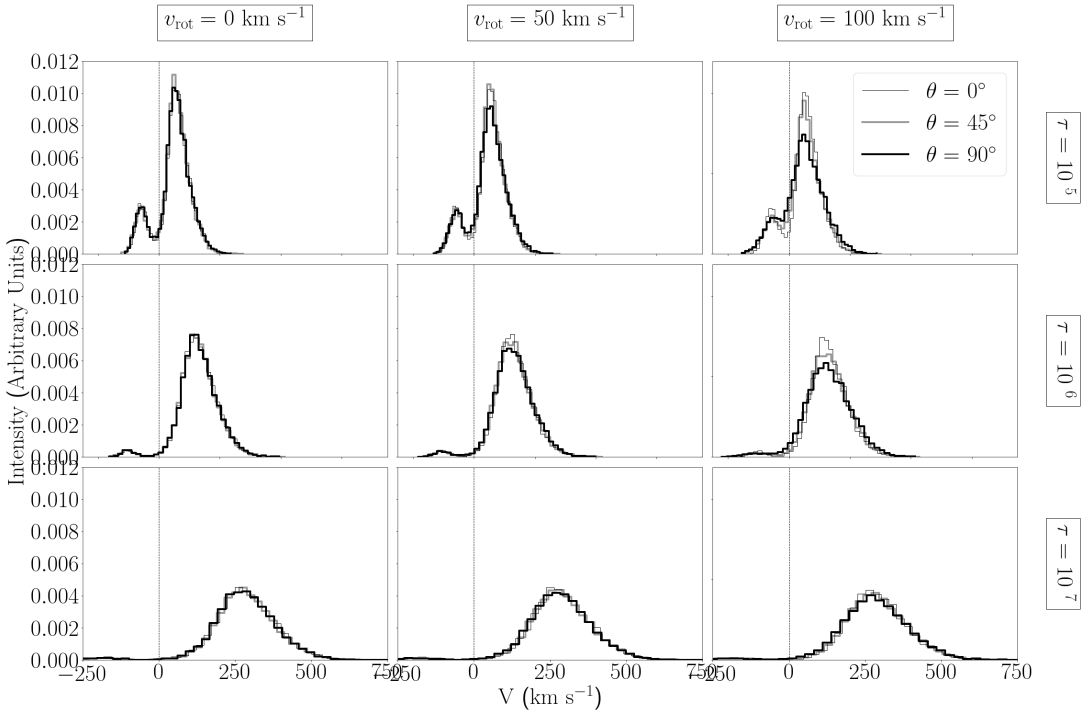

Figure A1. Caption: $v_{\rm out} = 50$km s^{-1}.

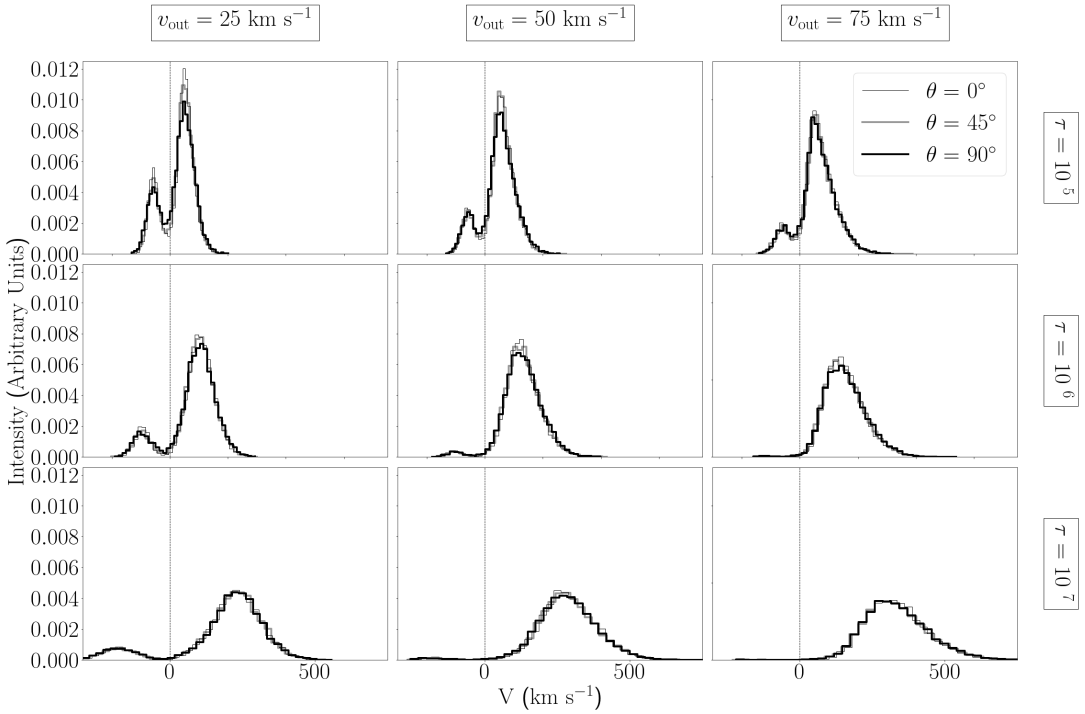

Figure A2. Caption: $v_{\rm rot} = 50$km s^{-1}.